

## Generation and healing of porosity in high purity copper by high-pressure torsion



Yuanshen Qi<sup>a,\*</sup>, Anna Kosinova<sup>a</sup>, Askar R. Kilmametov<sup>b</sup>, Boris B. Straumal<sup>b,c,d</sup>, Eugen Rabkin<sup>a,\*</sup>

<sup>a</sup> Department of Materials Science and Engineering, Technion – Israel Institute of Technology, 32000 Haifa, Israel

<sup>b</sup> Karlsruhe Institute of Technology, Institute of Nanotechnology, Eggenstein-Leopoldshafen, Germany

<sup>c</sup> National University of Science and Technology «MISIS», Moscow, Russia

<sup>d</sup> Institute of Solid State Physics, Russian Academy of Sciences, Chernogolovka, Russia

### ARTICLE INFO

#### Keywords:

High-pressure torsion  
Severe plastic deformation  
Porosity  
Copper  
Vacancy  
Diffusion

### ABSTRACT

Generation and healing of pores in metals under loading or during processing have long been important research topics, and their mechanisms are still debatable. In recent years, unexpected percolating networks of pores acting as ultra-fast diffusion paths were found in ultrafine-grained metals processed by severe plastic deformation. Herein, we conducted a systematic study of the mechanisms of generation and healing of pores in ultrahigh-purity copper (99.9995 wt%) during high-pressure torsion (HPT). In addition to a solid Cu disk, the disk with holes that were drilled before processing, resulting in nominal initial porosity of 4.48%, was processed by HPT. After HPT, the percolating porosities of  $0.07 \pm 0.01\%$  and  $0.04 \pm 0.01\%$  were found in the solid disk, and in the disk with pre-fabricated holes, respectively. Thus, higher initial porosity resulted in lower percolating porosity in the HPT-processed disk. Systemic characterization using scanning electron microscopy revealed that in both cases shear bands and ultra-fine grains are located in the regions with induced and healed pores. We discussed the mechanisms of porosity evolution in both cases. In the end, to verify the possibility of pores nucleation and growth by vacancy agglomeration, vacancy diffusivity during HPT processing was estimated. This work sheds a new light on the mechanisms of pores nucleation and evolution during severe plastic deformation.

### 1. Introduction

Generation and healing of pores in metals under loading or during processing have long been important research topics in physical and mechanical metallurgy. Evolution of pores or voids in bulk metallic materials has been extensively studied for better control of the ductile failure during plastic deformation [1]. It has been generally accepted that the generation of voids and their growth and coalescence are caused by high stress triaxiality under hydrostatic tension, i.e. the high value of the ratio of the mean stress to the equivalent stress [2,3]. On the contrary, hydrostatic pressure is essential for elimination of pre-existing voids. Studies have shown that porosity in as-cast metallic materials resulting from solidification can be eliminated by metalworking processes such as forging, rolling, etc. [4,5]. Evolution and healing of pre-existing porosity under plastic deformation has been studied using metal samples with artificially drilled holes [6]. It was found that hydrostatic pressure and shear strain enhance the collapse

and closure of pores and formation of sound bonding of the internal surfaces after they are brought into intimate atomic contact [6–9].

Hydrostatic pressure and shear strain are two indispensable features in most severe plastic deformation (SPD) techniques for producing ultrafine-grained metallic materials [10,11]. Moreover, the combination of ultrahigh hydrostatic pressure and simple shear allows consolidation of particulate materials to nearly full densification by eliminating porosity and building strong inter-particulate metallic bonding [12,13]. However, recent studies revealed that unexpected percolating porosity - a network of interconnected internal cavities, can be induced in bulk solid metallic samples during SPD processing, such as equal-channel angular pressing (ECAP) and high-pressure torsion (HPT) [14–19]. This is surprising, since a combination of high hydrostatic pressure and shear deformation imposed by SPD should supposedly lead to reduction of porosity. Therefore, one can conclude that the SPD processing may lead to two opposite impacts on the porosity evolution, i.e. simultaneous generation and healing of pores.

\* Corresponding authors.

E-mail addresses: [yuanshen.qi@technion.ac.il](mailto:yuanshen.qi@technion.ac.il) (Y. Qi), [anna.kosinova@technion.ac.il](mailto:anna.kosinova@technion.ac.il) (A. Kosinova), [askar.kilmametov@kit.edu](mailto:askar.kilmametov@kit.edu) (A.R. Kilmametov), [straumal@issp.ac.ru](mailto:straumal@issp.ac.ru) (B.B. Straumal), [erabkin@technion.ac.il](mailto:erabkin@technion.ac.il) (E. Rabkin).

<https://doi.org/10.1016/j.matchar.2018.08.023>

Received 10 April 2018; Received in revised form 3 August 2018; Accepted 13 August 2018

Available online 15 August 2018

1044-5803/ © 2018 Elsevier Inc. All rights reserved.

The percolating porosity induced by SPD was previously uncovered and quantified using radiotracer diffusion measurements [14,15]. Direct characterization of the pores in pure materials, regarding to their specific locations, morphologies and their effects on surrounding microstructures has not been systematically conducted. In addition, to the best knowledge of the authors, the efficiency of HPT in healing of pre-existing porosity has never been addressed.

To study both generation and healing of porosity during HPT process, two ultra-high purity copper disks, one in its bulk form and the other one with artificially drilled holes for introducing a pre-existing porosity were processed and characterized. Using electron microscopy characterization, the mechanisms of porosity generation and healing are analyzed. In the end, porosity formation is discussed in terms of accelerated vacancy diffusion during HPT.

## 2. Materials and Methods

Two high purity (99.9995 wt% or 5N5) Cu disks were processed by HPT at room temperature. One Cu disk of 10 mm in diameter and 0.7 mm in thickness was solid (in what follows “Cu disk”), while the other Cu disk of the same purity and dimensions had seven cylindrical holes of 0.8 mm in diameter drilled through the thickness (in what follows, “Cu-Holes disk”). One hole was located at the center and other six were located about 2.5 mm away from the center and 60° away from each other. Seven holes resulted in a porosity of 4.48%. The schematic illustration of the material and processing scheme is shown in Fig. 1. The HPT processing (5 anvil rotations at a rotation rate of 1 revolution per minute) was carried out under compressive pressure of 5 GPa in a Bridgman anvil-type unit with a quasi-constrained die using a custom-built computer controlled HPT device (W. Klement GmbH, Lang, Austria). After processing, the thickness of the disks decreased from 0.7 mm to ~0.4 mm and the diameter expanded from 10 mm to ~12 mm.

The microstructure characterization was conducted on the cross-section area of the disks. In what follows we assigned the labels normal direction (ND), shearing direction (SD), and transverse direction (TD) to the disk normal, to the in-plane direction in the cross-section orthogonal to ND, and to the out-of-cross-section direction, respectively (see Fig. 1). It should be noted, however, that the true shearing and transverse directions (SD' and TD') are the tangential and radial directions which change with respect to the location of the characterized regions. After processing, the disk was cut 3 mm away from its center and conventional sandwich specimens were made by gluing two Cu plates with similar sizes on each side of the sample, see Fig. 1. It is worth noting that after HPT 5 rotations under the pressure of 5 GPa, the microstructure of Cu samples of conventional purity should be homogeneous throughout the sample, both in radial and axial directions [20]. Epoxy was used to glue the two halves together and the curing was conducted on a hot plate at 120 °C for 20 min. Conventional

grinding using SiC paper down to 4000 grit and final mechanical polishing using 50 nm Al<sub>2</sub>O<sub>3</sub> suspension were conducted. Final electropolishing was carried out at room temperature in 14 M phosphoric acid by applying electric potential of 1.2 V. Time of about 2 min was sufficient to remove the damaged surface layer and reveal the grains. After electropolishing the samples were rinsed with distilled water. High resolution scanning electron microscopy (HRSEM) and electron back-scattered diffraction (EBSD) measurements were carried out using a Zeiss Ultra Plus SEM equipped with a Bruker EBSD detector. Three SEM imaging detectors were used to collect images for obtaining different information, namely a conventional secondary electron (SE) detector, an in-lens secondary electron detector, and a backscattered electron (BSE) detector. SEM in-lens images exhibit lower topographic and atomic number contrasts, but allow identification of pores with a better resolution than SEM-SE and BSE images [21]. Therefore, the volume fraction of pores was calculated based on the images acquired using in-lens detector. Focused ion beam (FIB) regular cross-section milling was carried out using a FEI Helios NanoLab DualBeam G3. For calculation of average grain size, twins and subgrains defined by the low-angle grain boundaries (LAGBs) with misorientation angle below 15° were not accounted for as individual grains. Moreover, average grain size was calculated based on area weight fraction, instead of number fraction.

## 3. Results

We characterized the distribution, morphologies, arrangement, and volume fractions of the pores in the as-cast material, in the HPT-processed Cu disk as well in the Cu-Holes disk. We also determined the grain size distribution and crystallographic orientations of the grains, paying special attention to the regions in the vicinity of induced pores and pre-existing holes.

### 3.1. Porosity Evolution

The grain boundaries (GBs) in the as-cast Cu sample (with the average grain size around 300 μm, see Ref. [22]) are decorated with small pores, as shown in Fig. 2(a, b). These pores have an average size of  $3.52 \pm 1.49 \mu\text{m}$  and make up  $0.07 \pm 0.01 \text{ vol}\%$  in the cross-section area. The volume fraction of the pore areas was determined by segmentation using ImageJ software. The threshold value was adjusted carefully in each image to ensure accuracy and the uncertainty in each measurement was about 0.01%. One representative segmented image is shown in Fig. 2(c). The formation of pores due to vacancy annihilation at the GBs during solidification is well-documented [23]. The micrometer dimensions of the pores are probably related to the high mobility of the vacancies owing to the extremely low impurity level. At melting temperature, the vacancy concentration is around  $10^{-4}$ , which exceeds by at least factor of 20 the concentration of impurities in the studied

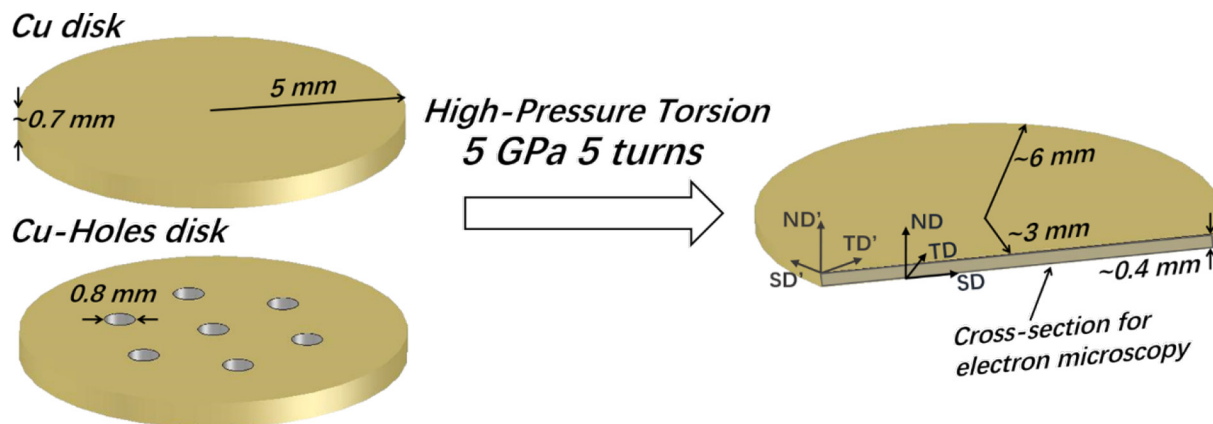


Fig. 1. Schematic illustration of the specimens and processing route. Note the difference between the coordinate systems (ND, SD, TD) and (ND', SD', TD').

Download English Version:

<https://daneshyari.com/en/article/8943222>

Download Persian Version:

<https://daneshyari.com/article/8943222>

[Daneshyari.com](https://daneshyari.com)